

HETEROCYCLES, Vol. 96, No. 10, 2018, pp. 1750 - 1758. © 2018 The Japan Institute of Heterocyclic Chemistry
Received, 7th August, 2018, Accepted, 10th September, 2018, Published online, 10th October, 2018
DOI: 10.3987/COM-18-13967

A NEW HBT-BASED FLUORESCENT PROBE FOR HYDRAZINE DETECTION IN AQUEOUS SOLUTION

Jing-Hua Dong,* Jia Deng, and Yuan Zhang

Hubei Collaborative Innovation Center for rare Metal Chemistry, Hubei Key Laboratory of Pollutant Analysis & Reuse Technology, College of Chemistry and Chemical Engineering, Hubei Normal University, Huangshi 435002, China.
E-mail: dongjh@hbnu.edu.cn

Abstract – A new HBT-based fluorescent probe is designed and synthesized for the detection of hydrazine based on Gabriel-type hydrazinolysis reaction mechanism. The probe responds selectively to hydrazine with obvious turn-on fluorescence. The water sample analysis indicated its great potential in the environment monitoring of hydrazine in aqueous solution.

INTRODUCTION

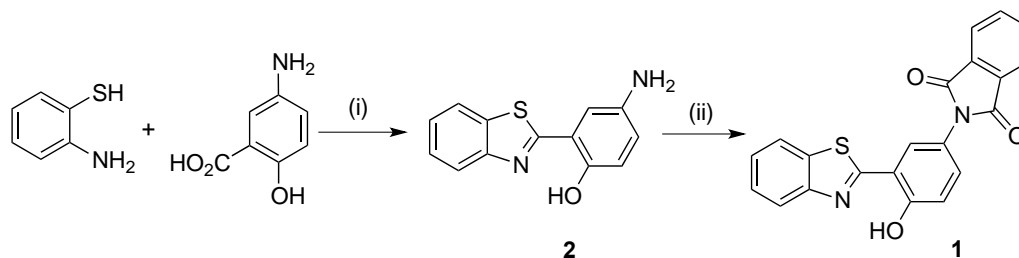
Hydrazine is widespread used as an important reactant in various chemical industries because of its high alkalinity and reducibility.¹ However, hydrazine can be readily absorbed by human bodies either orally or via skin penetration, leading to serious damages to organs and the central nervous system.^{2,3} As a result, hydrazine has been denoted as possible cancer-causing environmental contaminants.⁴ Therefore, it is highly needed to develop selective and sensitive methods for the detection of hydrazine in environmental and biological system.

Recently, fluorescent probe has gained increasing attention because of its simplicity, low cost, good selectivity, and high sensitivity.⁵ A number of fluorescent probes for hydrazine detection have also been reported.⁶ 2-(2'-Hydroxyphenyl)benzothiazole (HBT) is a well-known chromophore exhibiting excited state intramolecular proton transfer (ESIPT) through the keto-enol tautomerism which results in a large Stokes shift.⁷ Various HBT-based compounds as fluorescent probe have also been developed.⁸ However, HBT-based fluorescent probe for hydrazine is still rare.⁹ Here, we report a new HBT-based hydrazine fluorescence probe, 2-(3-(benzo[*d*]thiazol-2-yl)-4-hydroxyphenyl)isoindoline-1,3-dione (**1**). In probe **1**, HBT acts as a fluorophore for its excellent photophysical property, and isoindoline-1,3-dione linked to HBT as the hydrazine reaction site for hydrazine. Compared with the previous HBT-based hydrazine fluorescent probe,⁹ this new probe also shows high sensitivity and selectivity to hydrazine over other

related interfering species in aqueous solution. In particular, this new probe can be synthesized from cheap commercially available materials via a simple two-step reaction with good yield.

RESULTS AND DISCUSSION

The synthetic route of compound **1** was shown in Scheme 1. The structure of the probe **1** was determined by NMR, EI-MS (Figures S1-3), and elemental analyses.



Scheme 1. Synthetic route to **1**. Reagents and conditions: i) PPA, 150 °C, 12 h; ii) *o*-phthalic anhydride, AcOH, reflux, 5 h.

The UV-vis absorption and fluorescence emission spectra of probe **1** toward hydrazine were measured in HEPES buffer (10 mM, pH 7.0, 70% DMSO) at room temperature. As shown in Figure 1a, the free probe **1** showed the largest absorption band centered at 332 nm. Upon addition of 2.0 equiv. of hydrazine, the UV absorbance exhibits a large red shift from 332 nm to 403 nm. The fluorescence emission spectra of probe **1** toward hydrazine was shown in Figure 1b, the free probe **1** displayed a very weak emission ($\lambda_{\text{ex}} = 378$ nm). However, after addition of 2.0 equiv. of hydrazine, the significant increase of the fluorescence intensity at 523 nm and the fluorescent color changed from colorless to bright green can be observed. These results indicate the probe **1** can recognize the hydrazine.

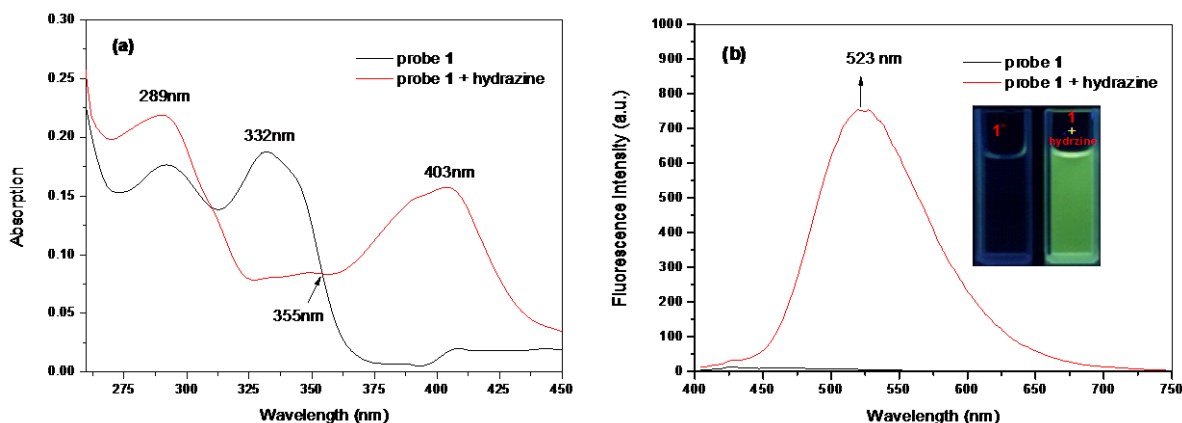


Figure 1. Absorption spectra (a) and Fluorescence spectra (b) of probe **1** (10.0 μM) upon addition of hydrazine (2.0 equiv.) in HEPES buffer (10 mM, pH 7.0, 70% DMSO) at room temperature. Insets in Figure 1b: fluorescent color changes of probe **1** upon addition of 2.0 equiv. of hydrazine ($\lambda_{\text{ex}} = 378$ nm).

To evaluate its sensing properties, the dynamics of the reaction between **1** (10 μM) in HEPES buffer (10 mM, pH 7.0, 70% DMSO) and hydrazine were studied by monitoring time-dependent fluorescence spectra. It can be seen from Figure 2, when 2.0 equiv. of hydrazine was added to the solution of the probe **1**, the emission intensity at 523 nm increased gradually over time and peaked within 60 min. As a result, the reaction time required to produce stable fluorescence intensity was 60 min.

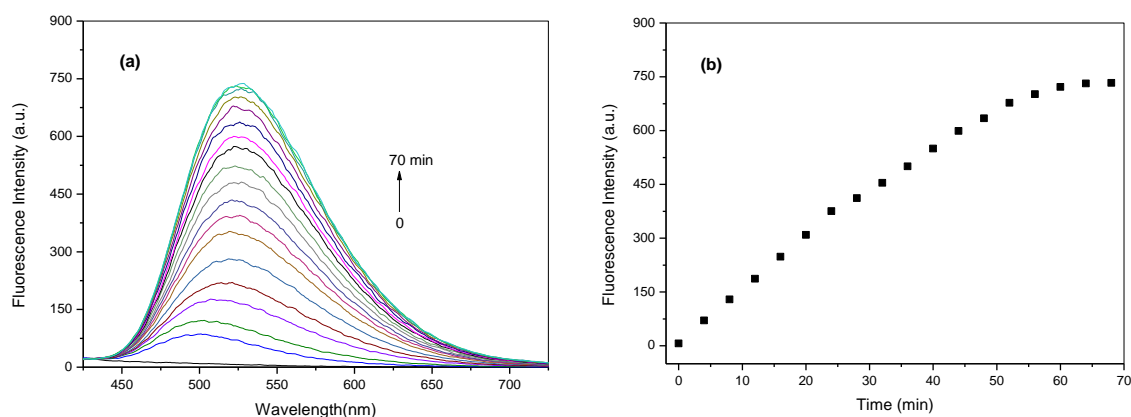


Figure 2. The fluorescence spectra of probe **1** (10 μM) incubated with hydrazine (2.0 equiv.) in HEPES buffer (10 mM, pH 7.0, 70% DMSO) at different reaction times (0–70 min) ($\lambda_{\text{ex}} = 378 \text{ nm}$) (a), and Time-dependent fluorescence intensity (523 nm) changes of probe **1** (10 μM) upon addition of 2.0 equiv. of hydrazine (b).

To evaluate the quantitative analysis of probe **1**, we further measured the absorption and fluorescence changes of probe **1** (10 μM) by increasing the hydrazine concentrations from 0 to 20 μM . As shown in Figure 3a, with increasing concentration of hydrazine, the absorption peaks of probe **1** (10 μM) at 332 nm was gradually decreased and at 289 nm was gradually increased, then a new band developed at 403 nm increased gradually. Two well-defined isosbestic points at 305 and 355 nm suggested the formation of a new substance. The concentration-dependent changes of the fluorescence spectra of probe **1** (10 μM) with hydrazine was shown in Figure 2b. Upon excitation at 378 nm, probe **1** exhibited an extremely weak fluorescence at 523 nm. The fluorescence quantum yield of probe **1** in the absence of hydrazine was calculated to be 0.025 with respect to rhodamine B in ethanol solution ($\Phi_{\text{u}} = 0.89$).¹⁰ The fluorescence intensity at 523 nm gradually increased with the addition of hydrazine (0–2.0 equiv.). The fluorescence quantum yield of **1** in the present of 2.0 equiv. of hydrazine was calculated to be 0.31, and an excellent linear relationship of emission intensity versus hydrazine concentration (0.6–2.0 equiv.) was observed ($R_2 = 0.9960$, $y = -286.0 + 556.2x$) (insert in Figure 2b). The detection limit of probe **1** is $2.13 \times 10^{-7} \text{ M}$ based on the definition of IUPAC ($C_{\text{DL}} = 3S_{\text{b}}/m$).¹¹ These results demonstrate that the probe **1** could be used to detect hydrazine quantitatively using the fluorescence spectroscopy method.

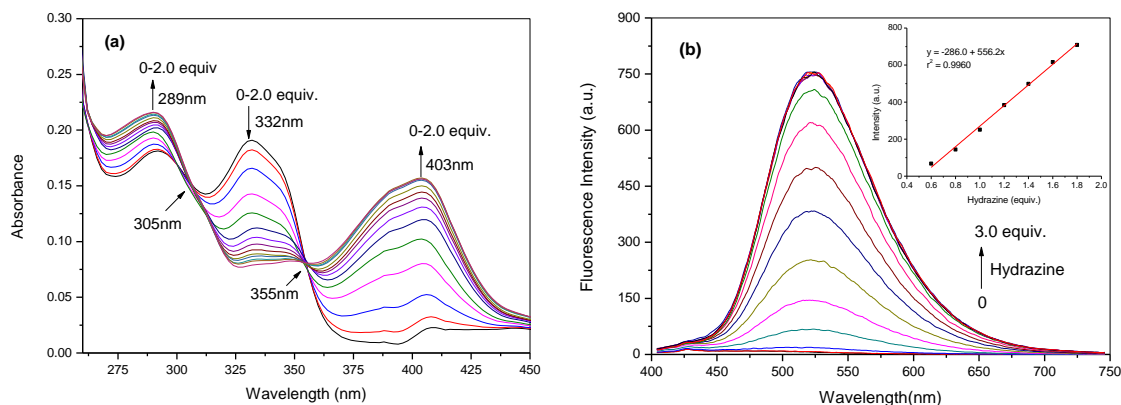


Figure 3. Absorption spectra (a) and fluorescence spectra (b) of probe **1** (10 μM) with the addition of increasing concentration of hydrazine (0–20 μM) in HEPES buffer (10 mM, pH 7.0, 70% DMSO) at room temperature. Insets in Figure 3b: linear relationship of emission intensity versus hydrazine concentration.

To evaluate the selectivity of probe **1**, we investigated the fluorescence response of **1** to various metal ions (Fe^{3+} , Cd^{2+} , K^+ , Na^+ , Mg^{2+} , Al^{3+} , Mn^{2+} , Cu^{2+} , Cr^{2+} , Co^{2+} , Zn^{2+} , and Ni^{2+}), anions (NO_3^- , HSO_4^- , H_2PO_4^- , Cl^- , Br^- , I^- , F^- , and ClO^-), and several common amine-containing species (ethylenediamine, diethylamine, triethylamine, ammonia, thiamine, urea, GSH, and Cys). As shown in Figure 4a, these interferences did not cause any noticeable fluorescence enhancement of **1** at 523 nm. Moreover, the competition experiments (Figure 4b) also indicated similar fluorescence responses of probe **1** to hydrazine in the presence or absence of various interferences. These results demonstrate that probe **1** can provide high specificity for hydrazine detection.

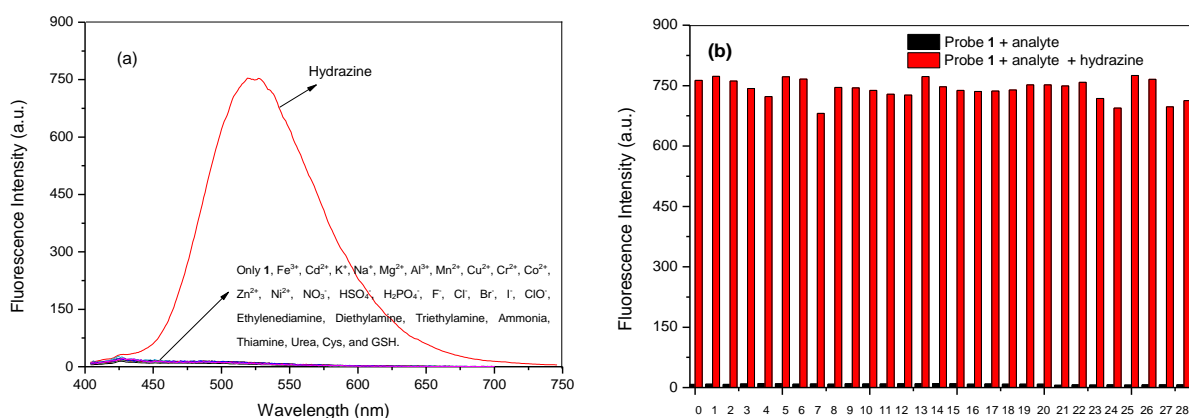
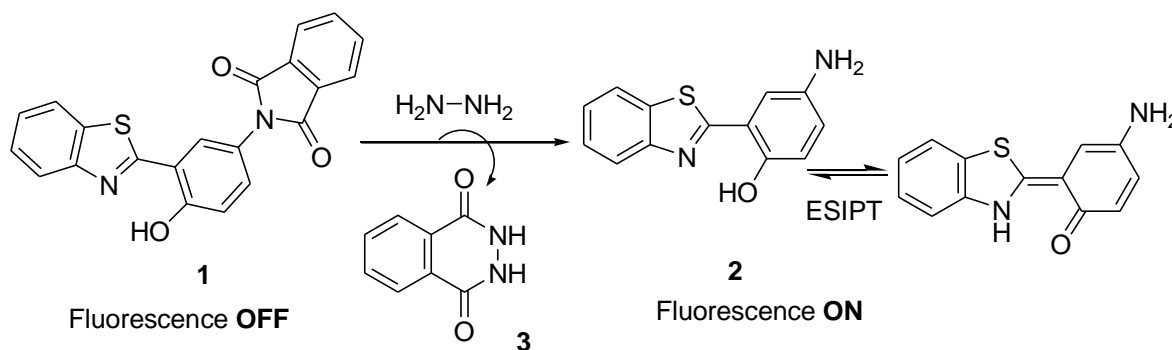


Figure 4. Fluorescence spectra of probe **1** (10 μM) upon addition of hydrazine (2.0 equiv.) and various cations, anions, and primary amines (10.0 equiv.) in HEPES buffer (10 mM, pH 7.0, 70% DMSO) at room temperature (a), and Fluorescence intensity at 523 nm of probe **1** (10.0 μM) upon addition of various analytes (10.0 equiv.) and then addition of hydrazine (2.0 equiv.). Black bar: probe **1** + various analytes. Red bar: probe **1** + various analytes + hydrazine. The excitation wavelength was 378 nm. (0. Blank, **1**, Fe^{3+} , 2. Cd^{2+} , 3. K^+ , 4. Na^+ , 5. Mg^{2+} , 6. Al^{3+} , Mn^{2+} , 7. Cu^{2+} , 8. Cr^{2+} , 9. Co^{2+} , 10. Zn^{2+} , 11. Ni^{2+} , 12. NO_3^- , 13. HSO_4^- , 14. H_2PO_4^- , 15. F^- , 16. Cl^- , 17. Br^- , 18. I^- , 19. ClO^- , 20. hydrazine, 21. ethylenediamine, 22. diethylamine, 23. triethylamine, 24. ammonia, 25. thiamine, 26. urea, 27. Cys, 28. GSH) (b).

To explore the sensing mechanism of probe **1** for hydrazine, the reaction products of probe **1** and hydrazine were separated and characterized. The fluorescence product and another one byproduct were characterized to be 4-amino-2-(benzo[*d*]thiazol-2-yl)phenol (**2**) and phthalhydrazide (**3**) by ESI-MS and NMR analysis, respectively (Figures S4-S8). Further studies were made by the absorption and fluorescence spectra of **2** in HEPES (10 mM, pH 7.0, 70% DMSO) at room temperature (Figures S9 and S10). The maximum absorption wavelength of **2** and its emission wavelength ($\lambda_{\text{ex}} = 378$ nm) is 378 nm and 523 nm, respectively, which is in agreement with the observed change of red-shift absorption spectra and turn-on emission spectra of probe **1** upon the addition of hydrazine (Figure 1). Therefore, a possible sensing mechanism based on the Gabriel reaction¹² was speculated in Scheme 2.



Scheme 2. Proposed sensing mechanism of probe **1** toward hydrazine.

Moreover, to better understand the optical responses of probe **1** reacting with hydrazine, electronic properties of ground state and excited state of **1** and compound **2** were also studied by DFT calculations at the B3LYP/6-31 G(d) level of the Gaussian 03 program. The optimized structure of probe **1** and its hydrazinolysis product **2** was shown in Figure 5, respectively. It can be seen from Figure 5b, the 2-(2'-hydroxyphenyl)benzothiazole (HBT) unit displays a co-planar configuration. However, the dihedral angle (139.0°) between isoindoline-1,3-dione and HBT unit indicated that probe **1** has a very big distortion, which maybe results in “turn-off” fluorescence. After hydrazinolysis of probe **1** with hydrazine, the fluorescence product, 4-amino-2-(benzo[*d*]thiazol-2-yl)phenol (**2**), a co-planar configuration molecule with ESIP effect was released into the solution and then the “turn-on” fluorescence change could be observed. Figure 6 shows the HOMO–LUMO orbital and energy level diagrams of probe **1** and compound **2**. As summarized in Figure 6, for compound **2**, the energy gap between the HOMO and LUMO was lower than that of probe **1**, which was in agreement with the red-shift in the absorption spectra.

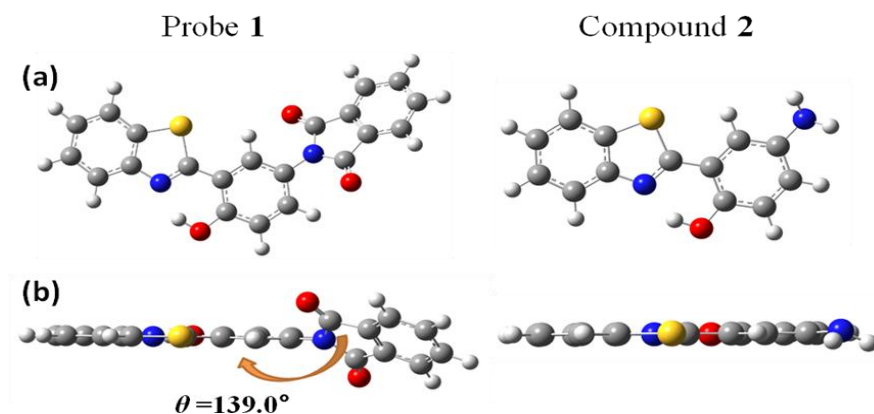


Figure 5. Top view (a) and side view (b) of the optimized structure of probe **1** (left) and compound **2** (right).

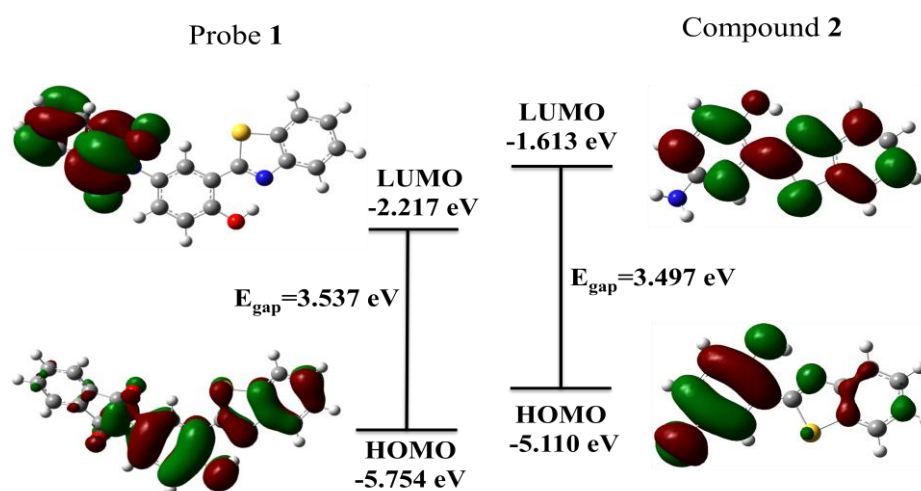


Figure 6. HOMO–LUMO orbitals of probe **1** (left) and compound **2** (right), and energy level diagrams of HOMO and LUMO orbitals of probe **1** and **2**, calculated on the DFT level using a B3LYP/6-31G* level of theory.

Hydrazine has been widely used in a various industrial processes. To evaluate the value of probe **1**, we also examined the function of probe **1** for its applications in real sample. Based on the experimental result shown in Figure 3, that is, when 2 equiv. of hydrazine was added, the fluorescence intensity of the solution of probe **1** (10 μM) reached maximum and then keep stable, The samples (distilled water, lake water and tap water sample) were spiked with 0, 4.0 μM , 8.0 μM , 16.0 μM and 20.0 μM of hydrazine and analyzed by proposed method.¹³ The study using the three water types showed that the presence of hydrazine can be well established up to a concentration of 20.0 μM (Figure 7). The results demonstrated that probe **1** can quantitatively detect hydrazine in real water samples.

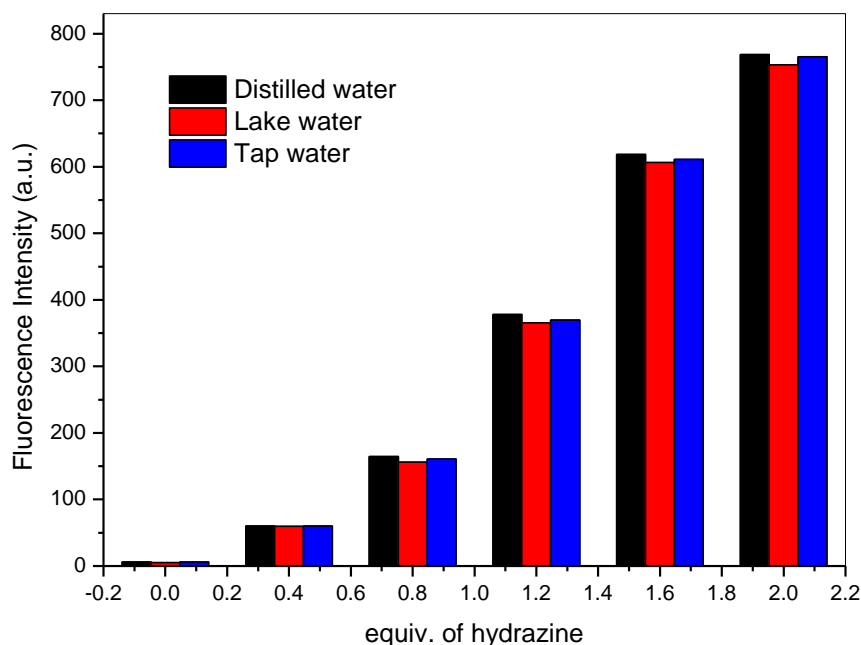


Figure 7. Fluorescence emission of probe **1** (10 μM) upon the addition of 0 μM , 4 μM , 8 μM , 12 μM , 16 μM , and 20 μM hydrazine in different water samples at room temperature with HEPES buffer (10 mM, pH 7.0, 70% DMSO).

In summary, a new and simple HBT-based fluorescent probe was designed and synthesized for hydrazine detection. The probe displayed distinct turn-on fluorescence changes upon addition of hydrazine. The detection limit was 2.13×10^{-7} M. The recognition mechanism is attributed to the Gabriel-type hydrazinolysis reaction. The water sample analysis indicated its great potential in the environment monitoring of hydrazine in aqueous solution.

EXPERIMENTAL

IR were recorded on a Perkin–Elmer PE–983 infrared spectrometer as KBr pellets with absorption in cm^{-1} . NMR was recorded on a Bruker 300 spectrometer with TMS as internal reference and CDCl_3 as solvent. Mass spectra were measured on a LCQ Advantage MAX (ESI). The elemental analyses were performed with a Vario EL-III instrument (Germany). UV spectra were measured on a SP-1900 spectrophotometer. Fluorescence spectra were determined on a Hitachi F-4500.

Reagents and Materials. 4-Amino-2-(benzo[*d*]thiazol-2-yl)phenol (**2**)^{7,8a} was synthesized by modified literature methods. Hydrazine monohydrate, other analytes and reagents used in this study were commercially available.

Synthesis of compounds 1: To a 25 mL flask containing acetic acid (8 mL), 4-amino-2-(benzo[*d*]thiazol-2-yl)phenol (**2**) (0.24 g, 1.0 mmol) and *o*-phthalic anhydride (0.15 g, 1.0 mmol) were added and the mixture was refluxed for 8 h. Then acetic acid was removed by reduce pressure and the

afforded solid was purified by column chromatography on silica gel to obtain **1** as a pale solid (0.28 g, 75%). IR (ν_{\max} , KBr, cm^{-1}): 3439, 2361, 1720, 1629, 1503, 1393, 1350, 1107, 754. ^1H NMR (CDCl_3 , 300 MHz): δ 7.43-7.56 (m, 2H), 7.51-7.56 (m, 1H), 7.77-7.83 (m, 3H), 7.90-7.99 (m, 1H), 8.00-8.04 (m, 3H), 12.75 (s, 1H); ^{13}C NMR (CDCl_3 , 75MHz): 117.1, 118.7, 121.6, 122.3, 123.2, 123.8, 125.8, 126.5, 126.8, 130.9, 131.7, 132.7, 134.5, 151.7, 157.6, 167.4, 168.4. ESI-MS: m/z 373.01 $[\text{M} + \text{H}]^+$. Anal. Calcd for $\text{C}_{21}\text{H}_{12}\text{N}_2\text{O}_3\text{S}$: C, 67.73; H, 3.25; N, 7.52. Found: C, 67.70; H, 3.21; N, 7.47.

General procedure for the spectra analysis

The stock solution of probe **1** in DMSO was diluted and pH of the solution was adjusted to about 7.0 using HEPES solution to deliver the final concentration of the probe (10 μM) in HEPES-DMSO (3:7, v/v) solution. Stock solutions of various metal ions, anions, hydrazine and other several common amine-containing species were prepared in deionized water. The optical spectra were recorded upon addition of analytes in HEPES buffer (10 mM, pH 7.0, 70% DMSO) at room temperature. For fluorescence tests, the excitation and emission slit width were 5 nm and 5 nm, respectively. Spectral data were recorded 60 min after the addition of analytes.

ACKNOWLEDGEMENTS

This study was supported by the 2017 open foundation of Hubei Key Laboratory of Pollutant Analysis & Reuse Technology (No. PA20170209).

REFERENCES AND NOTES

1. U. Ragnarsson, *Chem. Soc. Rev.*, 2001, **30**, 205.
2. C. A. Reilly and S. D. Aust, *Chem. Res. Toxicol.*, 1997, **10**, 328.
3. S. Garrod, M. E. Bollard, A. W. Nicholls, S. C. Connor, J. Connelly, J. K. Nicholson, and E. Holmes, *Chem. Res. Toxicol.*, 2005, **18**, 115.
4. G. Choudhary and H. Hansen, *Chemosphere*, 1998, **37**, 801.
5. For recent reports: (a) X. Li, X. Gao, W. Shi, and H. Ma, *Chem. Rev.*, 2014, **114**, 590; (b) J. Ma, L. Yan, B. Chen, and M. Sun, *Heterocycles*, 2018, **96**, 850; (c) X. Wang, D. Jin, X. Li, X. Yan, and B. Wang, *Heterocycles*, 2018, **96**, 707; (d) F. Zhang, Y. Hu, Q. Li, and S. Hu, *Heterocycles*, 2017, **94**, 515.
6. For recent reports: (a) M. H. Lee, B. Yoon, J. S. Kim, and J. L. Sessler, *Chem. Sci.*, 2013, **4**, 4121; (b) B. Shi, Y. He, P. Zhang, Y. Wang, M. Yu, H. Zhang, L. Wei, and Z. L., *Dyes Pigm.*, 2017, **147**, 152; (c) X. Zheng, S. Wang, H. Wang, R. Zhang, J. Liu, and B. Zhao, *Spectrochim. Acta A*, 2015, **138**, 247; (d) L. Wang, F. Liu, H. Liu, Y. Dong, T. Liu, J. Liu, Y. Yao, and X. Wan, *Sens. Actuators B: Chem.*, 2016, **229**, 441; (e) J. Zhou, R. Shi, J. Liu, R. Wang, Y. Xu, and X. Qian, *Org. Biomol.*

- [Chem.](#), 2015, **13**, 5344; (f) Y. D. Lin and T. J. Chow, *RSC Adv.*, 2013, **3**, 17924.
7. K. Anthony, R. G. Brown, J. D. Hepworth, K. W. Hodgson, B. May, and M. A. West, *J. Chem. Soc., Perkin Trans. 2*, 1984, 2111.
 8. For recent reports: (a) Y. Pan and Y. Han, *Tetrahedron Lett.*, 2017, **58**, 1301; (b) M. Santra, B. Roy, and K. H. Ahn, *Org. Lett.*, 2011, **13**, 3422; (c) S. Goswami, A. Manna, S. Paul, K. Aich, A. K. Das, and S. Chakraborty, *Tetrahedron Lett.*, 2013, **54**, 1785; (d) X. J. Liu, Q. W. Yang, W. Q. Chen, L. N. Mo, S. Chen, J. Kang, and X. Z. Song, *Org. Biomol. Chem.*, 2015, **13**, 8663; (e) D. Kand, P. S. Mandal, A. Datar, and P. Talukdar, *Dyes Pigm.*, 2014, **106**, 25; (f) Y. C. Wu, J. P. Huo, L. Cao, S. Ding, L.Y. Wang, D. R. Cao, and Z. Y. Wang, *Sens. Actuators B: Chem.*, 2016, **237**, 865.
 9. Z. Chen, X. Zhong, W. Qu, T. Shi, H. Liu, H. He, X. Zhang, and S. Wang, *Tetrahedron Lett.*, 2017, **58**, 2596.
 10. X. Yang, Z. T. Pan, and Y. Ma, *J. Anal. Sci.*, 2003, **19**, 588 (in Chinese).
 11. B. P. Joshi, J. Park, W. I. Lee, and K. H. Lee, *Talanta*, 2009, **78**, 903.
 12. R. Maji, A. K. Mahapatra, K. Maiti, S. Mondal, S. S. Ali, P. Sahoo, S. Mandal, M. R. Uddin, S. Goswami, C. K. Quah, and H. K. Fun, *RSC Adv.*, 2016, **6**, 70855.
 13. S. Goswami, K. Aich, S. Das, S. Basu Roy, B. Pakhira, and S. Sarkar, *RSC Adv.*, 2014, **4**, 14210.